International Journal of Advances in Engineering and Management (IJAEM)
Volume 2, Issue 6, pp: 571-578 www.ijaem.net ISSN: 2395-5252

Role of Grain Size in Sensitization on 316l Stainless Steel

T. N. Suresh Kumar [1], Dr. T. Anand [2], Shorn Philip [3], Raghul. N [4], Dinesh. G [5]

[1]Associate professor,[2] Professor, Department of mechanical and automation Engineering, Agni college of Technology, Thalambur, Chennai-130

[3,4,5] Students, Department of mechanical and automation Engineering, Agni college of Technology, Thalambur, Chennai-130

Corresponding author: T. N. Suresh Kuma

Date of Submission: 15-09-2020 Date of Acceptance: 26-09-2020

ABSTRACT—Sensitization is the loss of composite uprightness. It results from chromium consumption in the region of carbides accelerated at grain limits. This makes the steel or combination become defenseless to intergranular consumption or intergranular stress erosion breaking (SCC). Certain composites when introduced to a temperature depicted as a honing temperature become particularly feeble to intergranular utilization. This is depicted by a constrained attack at and neighboring grain limits with commonly little utilization of the grains themselves. The composite falls apart (grains drop out) or possibly loses its quality. Subsequently the investigation in refinement is made to decrease the intergranular consumption and to analyze the grain limits and grain size with the IGC. For this procedure, 316L Stainless steel material is picked where this activity draws out the job of grain size in refinement of 316L tempered steel. At first the tempered steel is warmed to 1200^0C and is water extinguished right away. Arrangement of procedure is accomplished for example and hot moving to decide the misshaping of the material. The grain size of the material is recognized by utilizing a Scanning Electron Microscope (SEM). Thus, after a progression of procedure and testing it dra ws out that the Grain size Increases when the decrease is least for 60% there are no grain development and at the level of moving increments where the Grain size reductions.

Keywords—Sensitization, Rolling, SEM (scanning electron microscope), Heat Treatment

I. INTRODUCTION

Austenitic Stainless Steels (ASS) have incredible protection from general consumption. They are, in any case, inclined to confined consumption – cleft and pitting erosion, intergranular consumption (IGC) and stress erosion splitting (IGSCC). The two types of limited erosion, IGC and IGSCC, are frequently brought about by sharpening - however the equivalent can likewise be brought about by isolation of dynamic components. Sharpening is normally made when an ASS is welded or heat rewarded for adequate time in the temperature scope of 500-
800^0C, which prompts precipitation of chromium rich carbides at the grain limits.

Development of such carbides can prompt the arrangement of chromium drained zones in the quick encompassing Other than the control of science, refinement can likewise be controlled through upgrading grain limit nature and grain size. The grain

limit nature is frequently recognized from the incidental site cross section (CSL) hypothesis. It is the main way, at any rate by and by, to relate tentatively got neighborhood direction estimations with grain limit nature or vitality.

However, such a characterization stays a long way from definite. Despite such limitations, the general comprehension was 'nearness of irregular, non CSL-high-edge limits are inconvenient to neighborhood erosion opposition'. The influence of recrystallized structure and texture on the sensitization behavior of a stable austenitic stainless steel (AISI 316L) in the eff ects of an n ealin g and cold rol lin g on th e sensitization–desensitization behavior of AISI 316L stainless steel and its susceptibility to intergranular corrosion have been studied by electrochemical potentiokinetic reactivation (EPR) tests. The

International Journal of Advances in Engineering and Management (IJAEM)
Volume 2, Issue 6, pp: 571-578 www.ijaem.net ISSN: 2395-5252

results indicate that the reco vered stru cture as well a s th e recrystallized structure show different sensitization behavior. Growth of the grains shows poor sensitization behavior. The role of the texture and the grain boundary character distribution (GBCD) on the sensitization process has also been discussed **[1]**.

Sensitization behavior of modified 316N and 316L stainless steel weld metals after complex annealing and stress relieving cycles. Sensitization behavior of austenitic stainless-steel weld metals prepared using indigenously developed modified electrodes was studied. Detailed optical and scanning electron microscopic examination was carried out to understand the microstructural changes occurring in the weld metal during isothermal exposure at various temperatures r anging from 500 °C to 850 °C

Based on these studies the mechanism of sensitization in the austenite–ferrite weld metal has been explained The heating/cooling rates to be followed for avoiding sensitization during heat treatment cycles consisting of solution-annealing and stress-relieving in fabrication of welded components of AISI
316LN stainless steel (SS) were estimated considering the soaking time and the number of times the component undergoes thermal excursions in the sensitization regime. The results were validated by performing controlled heating and cooling heat treatment trials on welded specimens **[2]**.

An orderly examination of the impact of time and temperature in the refinement of hardened steel AISI 304L, AISI 316L, AISI 321 and AISI 347 funnels utilized in oil refining plants. The refinement was evaluated by SEM as indicated by ASTM A-262 and by the Double Loop Electrochemical Potentiokinetic Reactivation test (DLEPR). The outcomes indicated that all prepares didn't present sharpening at working temperature in the desulfurizer's procedure, yet the temperature of 500℃ was basic to the showing up of refinement for the both low carbon hardened steels and AISI 321 SS, while for the AISI 347 the basic temperature was 550℃. The balanced out prepares affirmed to be more impervious to sharpening than the low carbon hardened steels, and niobium demonstrated to be more proficient settling operator than titanium **[3]**.

The pitting consumption and sharpening in laser quick produced examples of type 316L tempered steel are considered and contrasted and its fashioned and weld store partners. Concerning fashioned examples, the laser quick made examples displayed lower pitting erosion obstruction just as further extent of refinement. Notwithstanding, pitting erosion opposition of laser fast fabricated examples is to a great extent like that of PTAW-stored during different layer statement combined with slower pace of cooling during later piece of laser quick assembling brought about refinement, offering ascend to consistent erosion assault along the grain limits **[4]**.

Sharpening conduct of austenitic treated steel weld metals arranged utilizing indigenously created altered 316N anodes was considered. Point by point optical and checking electron infinitesimal assessment was completed to comprehend the microstructural changes happening in the weld metal during isothermal introduction at different temperatures Time–temperature–refinement outlines were built up utilizing ASTM A262 Practice E test. From the TTS charts, basic cooling rate above which there is no danger of refinement was determined for the two materials **[5]**.

Electrochemical potentiokinetic reactivation procedure (EPR) was utilized to survey level of sharpening in 316L hardened steel dispersion fortified joint. The outcome indicated the level of refinement of DBJ was a lot littler than that of base material (BM). No chromium carbides accelerated at grain limits in DBJ after 100 h treatment at 650 ℃, while chromium carbides could be seen unmistakably in the BM after 8 h treatment, demonstrating that DBJ has preferred intergranular consumption opposition over BM **[6]**.

Laser surface softening of sharpened nitrogen -bearing sort 316L austenitic tempered steel was completed utilizing a beat ruby laser. The sharpening heat treatment was done. The level of refinement was surveyed by the electrochemical potentiokinetic reactivation (EPR) test. The basic pitting possibilities of as-sharpened just as sharpened laser liquefied examples were controlled by potentiodynamic anodic polarization technique in a medium containing at room temperature. Results showed that upon laser softening the pitting obstruction expanded essentially. This expansion was ascribed to the disposal of the sharpened heterogeneous microstructure by laser dissolving. The minuscule assessment of the hollowed examples indicated just micropits that created at the interfaces of oxide/sulfide incorporations of titanium and framework **[7]**.

The working states of this test were at first enhanced utilizing the trial structure technique on the bases of the dependability, the selectivity, and the reproducibility of test reactions for both toughened and sharpened prepares. The TTS

International Journal of Advances in Engineering and Management (IJAEM)
Volume 2, Issue 6, pp: 571-578 www.ijaem.net ISSN: 2395-5252

chart of the AISI 316L treated steel was built up utilizing this strategy. This outline offers a quantitative appraisal of the DOS and a likelihood to value the time-temperature equality of the IGC refinement and desensitization. (3) The diagnostic strategy dependent on the chromium dispersion models **[8]**.

The precipitation conducts and sharpening opposition of Type 316L(N) tempered steels containing various centralizations of nitrogen have been examined at the maturing state of 700℃ for cold work (CW) levels. Nitrogen in the disfigured combinations impeded the between and intra-granular precipitation of the carbides at low and high CW levels individually, while it expanded the overall measure of the χ stage. Quantitative evaluation of the level of refinement (DOS) utilizing the twofold circle electrochemical potentiokinetic reactivation (DL-EPR) tests showed that CW levels up to 20% improved sharpening while 40% CW stifled refinement for every maturing time. The expansion in nitrogen content quickened the refinement at CW levels beneath 20%. This may be related with the homogeneous dispersion of separations and the lower propensity toward recrystallization showed in the composites having higher nitrogen content **[9]**.

Quantitative evaluation of the level of refinement (DOS) utilizing the two fold circle electrochemical potentiokinetic reactivation tests showed that levels up to 20% improved sharpening while stifled refinement for every maturing time. The expansion in nitrogen content quickened the refinement at CW levels beneath 20%. This may be related with the homogeneous dispersion of separations and the lower propensity toward recrystallization showed in the composites having higher nitrogen content **[10]**.

II. EXPERIMENTAL DETAILS

The property or the assistant headways of any crystalline material depend upon the size, shape and transport of grains or organizes and moreover on their headings. The past is a scalar sum: assessing it is commonly basic. The course is a 3X3 matrix: genera lly described as the go essential to blend the model (or reference, for instance, moving, transverse and customary headings) and the valuable stone co-ordinate system. This is addressed as Euler point, plant administrator documents or rotate edge pair, or graphically in shaft figures and in reverse post. The miniaturized scale surface addresses such course and moreover the spatial zone (or exact position/co-ordinate in microstructure). Addressing such micro texture headings as discrete centers is possible just if the amounts of centers are confined. An 'averaging' is required something different.

$$\frac{V_g}{V} = f(g)\, dg \qquad (1)$$

Where, Vg is the volume of an orientation g
V is the total volume. Clearly f (g), the so-called randomness number, is a measure of 'average' orientation-strength of g and serves as the basis of ODF.
Naturally ODF calculation involves much more than the simple schematic of fig.1 explains Both texture and crystallographic symmetries.

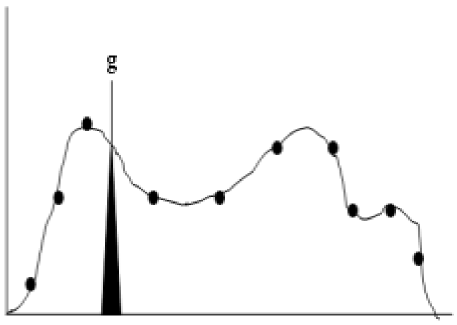

Fig. 1. ODF of Texture and crystallographic

2.1. MATERIAL SELECTION

AISI 316L austenitic stainless-steel material is chosen for the experiment. The material is cut with a dimension of 1.5x10 cm. The material is then heat treated at a temperature of 1050-1200℃ in a furnace for 60 minutes. It is removed from the furnace and immediately water quenched. The sample undergoes hot rolling process with various reduction of 20%, 60%, 80%. Finally, the Role of grain size and boundaries is observed using a Scanning Electron Microscope.
The selected material 316L SS is shown in the fig.2.


Fig. 2. AISI 316L SS

ASS type 316 L was used in the present study. The chemical composition of the material

International Journal of Advances in Engineering and Management (IJAEM)
Volume 2, Issue 6, pp: 571-578 www.ijaem.net ISSN: 2395-5252

is shown in the Table 1

Table 1. Chemical composition of 316L SS (%)

Material	C	S	P	Si	Mn	Cr	Ni	Mo	Cu	N
316L(%)	0.025%	0.05%	0.024%	0.44%	1.59%	17.15%	11.73%	2.70%	0.234%	0.2%

We use 316L SS material because the Hardened steel are austenitic containing molybdenum, expanding their protection from various substance corrodents and marine situations. 316L are a hardened steel extra low carbon variation. These materials are more safe than standard austenitic treated steels to general consumption and pitting/fissure. They likewise give progressively critical drag, worry to-burst and elasticity at high temperatures, fantastic protection from erosion and quality attributes, and are appropriate for fabricated or molded applications.

Type 316 L treated steel is a variant of the 316 steel amalgams with additional low carbon. As an outcome of welding, the diminished carbon content in 316 L limits destructive carbide precipitation. To ensure most extreme erosion opposition, 316 L is utilized when welding is required.

At room temperature, Grade 316 stainless steel also exhibits the properties of 316L stainless steel is given in Table 2.

Table 2. Properties of 316L Stainless steel

Density	99 g/cm3
Thermal Expansion	9 mm/m/°C
Electrical Resistivity	4 μohm/cm
Thermal conductivity	3 W.m-1. °K-1
Modulus of elasticity	193 GPa

SAMPLE TESTING

3.1. SPECIMEN PREPARATION

Wire electrical discharge machining (EDM) is a process of metal machining in which a tool discharges thousands of sparks to a metal workpiece as shown in fig.3.

A non-conventional process, wire EDM works on parts resistant to conventional machining processes, EDM melts or vaporizes it, leaving little debris and providing a very accurate line. After the process the obtained material is shown in fig.4.

Fig. 3.EDM Machine Fig. 4. Material obtained After machining

3.2. HEAT TREATMENT

The material is heated at a temperature of 1200 C in a box furnace as shown in fig.5 below for 60 minutes. The maximum temperature that the furnace can reach is 1400 C. It takes about 10 minutes for the furnace to reach a temperature of 1200 ºC.

Fig .5. Box furnace

3.3. H OT R OLLING

Sample plate is cut into small pieces at 10 cm×10 cm×20cm m. After Water Quenching process, the speci men is subjected to at Standard ASTM A240. Heat treatment process is followed by which the specimen Is placed in the furnace for 60 mins at 12000C. After 60 minutes water quenching is to be done, where in this 12 samples minimum 3 pieces are selected and these three pieces are subjected to Hot rolling, after completing this process we go for analysis work 30% Hot Rolling in Unidirectional and cross directional.

After the Sensitization and rolling process the speci men is anal yzed using SEM and X-R ay ODFs. The material obtained after the rolling process is shown in the fig 7 and the machi ne used for the rolling process is shown in the fig 6.

International Journal of Advances in Engineering and Management (IJAEM)
Volume 2, Issue 6, pp: 571-578 www.ijaem.net ISSN: 2395-5252

Fig. 6. Rolling machine **Fig. 7.**Material obtained After rolling

III. PROCESS FLOWCHART

The process which is been held is decribed in a flow chart step by step for better understanding as shown in fig.8.

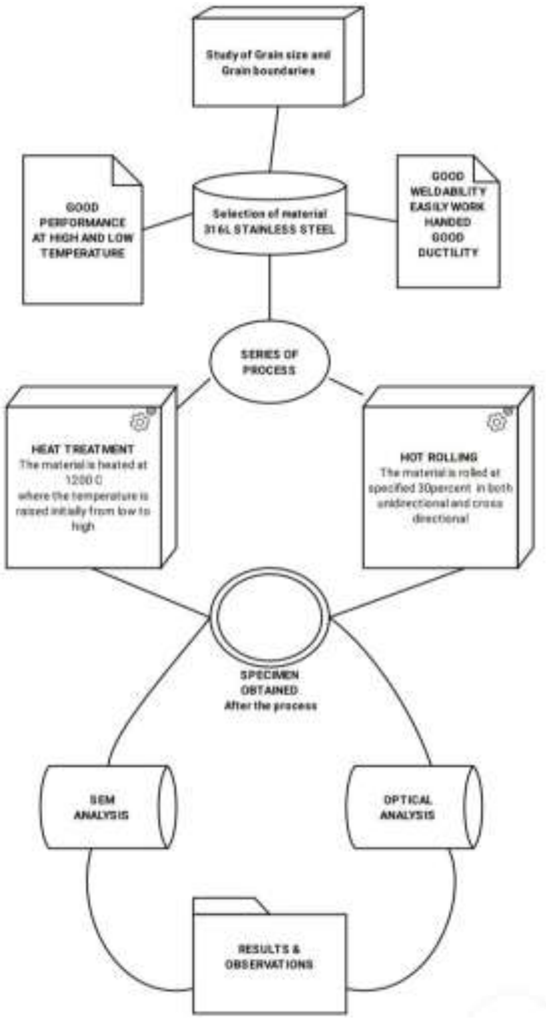

Fig .8. Process flow chart

IV. RESULTS AND DISCUSSION

5.1. GRAIN BOUNDARY CHARACTER DISTRIBUTION (GBCD)

The mass surface outcomes, as portrayed in the past section, may not be adequate to reach determinations with respect to the sort and relative measure of grain limits that are available in the examples. For such reasons neighborhood direction estimations, utilizing Orientation Imaging Microscopy (OIM), were completed. Although, as clarified over, this procedure isn't great, it permits us to get a factually significant arrangement of information in a sensible time. In the solutionized210 tests of both the evaluations, two OIM outputs of in any event 200x200 µm have been recorded. Curiously, no critical distinction was found in the overall measure of low point limits (misorientations between 1-10°; 1° is considered as the exactness of OIM estimations and this deformation of CSL is shown in fig .9.

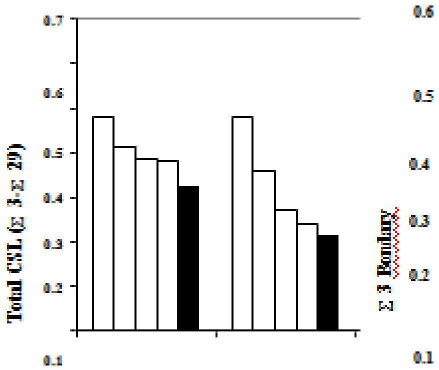

Fig .9. Deformation of CSL 316L percentage

The effect of pre-solutionizing deformation on CSL boundary fraction - (a) 3-29 and (b) Both fractions were estimated using Brandon's criteria, with the angular deviation from exact CSL and the type of CSL. U and CR stand respectively for pre-solutionizing unidirectional rolling and cross rolling .The rolling percentage has been shown in Table 3.

International Journal of Advances in Engineering and Management (IJAEM)
Volume 2, Issue 6, pp: 571-578 www.ijaem.net ISSN: 2395-5252

Table 3. Rolling percentage (Unidirectional & Cross Rolled)

Pre-solutionizing Reduction Percentage	0%	20%	40%	60%	80%
Type 316L SS					
Unidirectional Rolled	60%	75%	75%	55%	45%
Cross Rolled	60%	49%	45%	40%	35%

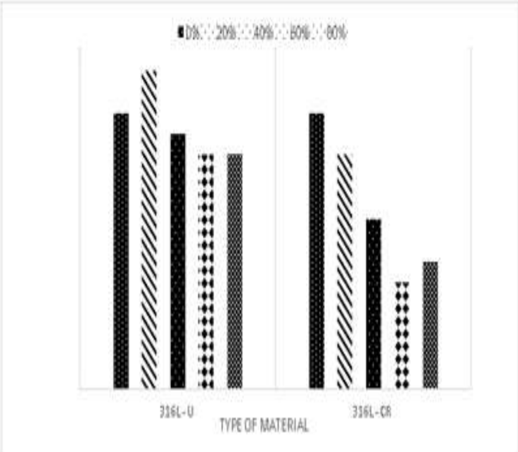

Fig.10. Deformation percentage before rolling

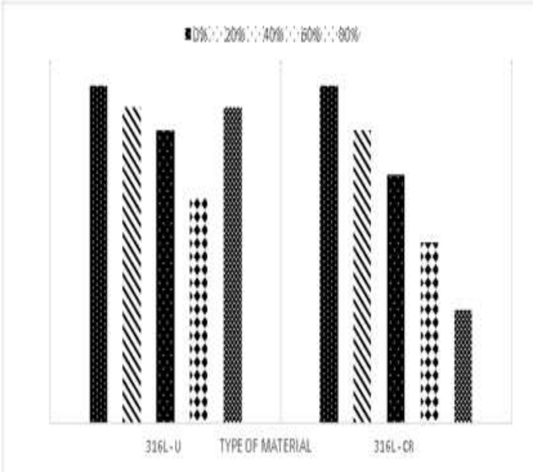

Fig .11. Deformation percentage after rolling

The observed trends in CSL boundary nature with respect to pre- solutionizing deformation can be summarized as a drop in both and 3-29 fractions with increasing deformation percentage as shown in fig.10 and fig .11 the same trend is found in both the grades and under both unidirectional land cross-rolling - the fraction of with unidirectional rolling also dropped in all cases, except for type 316L Except for type 316L stainless steel under unidirectional rolling, the perfection of both and 3-29 dropped at increasing reduction percentages. The effect of pre-solutionizing deformation can be generalized as an 'Effective Grain Boundary Randomization', as illustrated by figures 10 and 11, indicating a stronger presence of so-called random boundaries at higher reduction percentages .These numbers of the average grain sizes will be subsequently used for explaining and elaborating the DOS and IGC results.

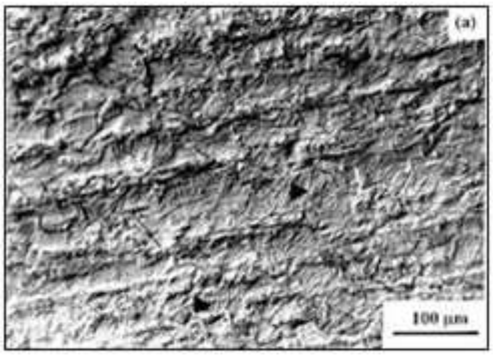

Fig.12. Type 316L 40% unidirectional rolled

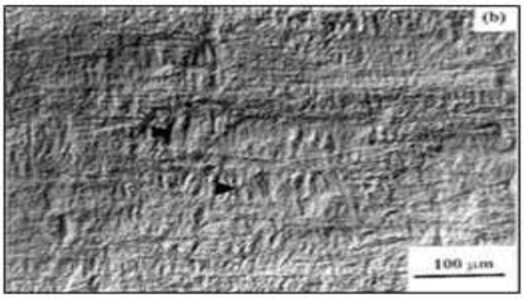

Fig .13. Type 316L 80% unidirectional rolled

Optical microstructures of deformed austenitic stainless steels of 316L is shown in fig.12 and fig.13 with 40% and 80% unidirectional All pictures were taken from the mid-thickness section of the rolling plane, containing rolling (RD) and transverse (TD) directions – the latter being apparent from relative elongation of the grains. It is to be noted that the undeformed grains sizes were 71 and 50 respectively for type 316L stainless steel. Certain interesting features (involving apparent grain splitting and strain localizations) are marked with arrow-heads (a) Relative changes in significant surface segments, during disfigurement of 316L hardened steel. The relative changes were distinguished from the inclines as shown in Table 4.

International Journal of Advances in Engineering and Management (IJAEM)
Volume 2, Issue 6, pp: 571-578 www.ijaem.net ISSN: 2395-5252

(b) Average (for both unidirectional and cross moving) values for Brass and Copper + S are given for 316L treated steel as shown in Table 5.

Table 5 . Orientation for Unidirectional & Cross Rolling

Major Orientations	Type 316L SS	
	Unidirectional Rolling	Cross Rolling
Taylor {4 4 11} <118>	-0.005	0.003
Brass {011} <211>	-0.008	0.006
S {231} <346>	0.080	0.080
Copper {112} <111>	0.055	0.044
CG {012} <100>	-0.030	-0.032
CH {001} <210>	-0.056	-0.065

Table 5. Orientation for Brass & Copper + s

Orientation	Type 316L SS
Brass	0
Copper + S	0.070

5.2. DEFORMATION OF GRAIN SIZE

X-ray ODFs of the material after annealing were obtained by the standard series expansion method using the program MTM- FHM. shows the as-received undeformed material with maximum ODF intensity, hot reduction substantially increased the texture-maximum ODF at 70%.

The result of ODFs, have been further elaborated in terms of volume fractions of major texture components. The major texture components were identified from the usual ideal fcc texture components with, an average, more than 5% volume (approximate limit for effective X-ray detection).

The changes in the texture components, with increasing percentage reduction, was assumed to be linear and the trends of such changes were estimated from the slope. As given copper had more significant increase. This change of texture components at different ODFs are shown in fig.12.

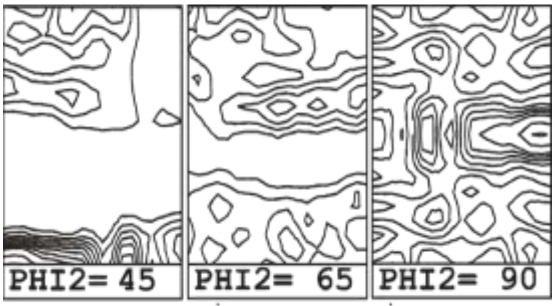

Fig .12. X-ray ODFs of type 316L stainless steel (Undeformed as-received)

V. CONCLUSION

The study in sensitization is made in order to reduce the intergranular corrosion and to examine the grain boundaries and grain size with the IGC. For this process, 316L Stainless steel material is chosen where this job brings out the role of grain size in sensitization of 316L stainless steel. Initially the stainless steel is heated to 1200^0C and is water quenched immediately. Series of process is done for instance and hot rolling to determine the deformation of the material. The grain size of the material is identified by using a Scanning Electron Microscope (SEM). As a result, after a series of process and testing it brings out that The Grain size Increases when the reduction is minimum for 60% there are no grain formation and the percentage of rolling increases where the Grain size decreases. This is examined from the SEM image as shown in fig.13

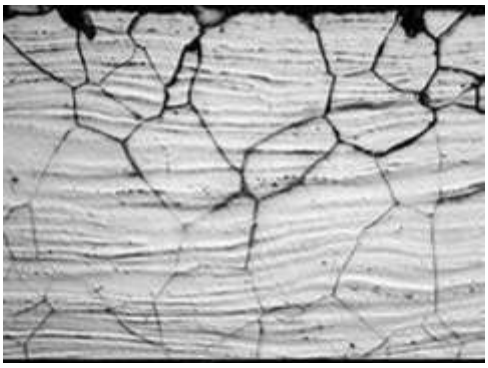

Fig.13. Obtained SEM image

The growth of chromium rich carbide(s) at the grain boundaries requires a supply of chromium from the surrounding matrix. The boundary may act as a 'collector-plate' around such grain boundary carbides [212,213]. With the Cr depletion in the neighborhood, the ASS may eventually become sensitive to IGC [198], caused by the chemical and physical differences between the grain boundaries and their immediate surroundings. This is common in welded structures, where thermal history may create conditions suitable to sensitization [195,209-211]. Modifications in chemistry (e.g. lowering of carbon and/or additions of strong carbide formers) and/or suitable heat treatments [195,209-211] are the usual means of reducing sensitization and hence IGC.

REFERENCES

[1]. Sandip Ghosh Chowdhury & Raghuvir Singh, Recrystallize structure and texture on sensitization of SS316Lin the Scripta materialia of Metallurgical and Materials Transactions A 37(8):2349-2359.

[2]. D.N. Wenski & V. Kain & B. Verlinden, Resistance to sensitization and intergranular corrosion in Acta materialia, Volume 50, Issue 18, 28 October 2002, Pages 4587-4601.

[3]. A. S. Lima, A. M. Nascimento, H. F. G. Abreu & P. de Lima- Neto proposed the Sensitization evaluation of the austenitic stainless steel AISI 304L, 316L, 321 and 347 in the Journal of Materials Science volume 40, pages139–144(2005).

[4]. P.Ganesha Raju Girib, R. Kaula P. Ram Sankara PragyaTiwariho kAtulkarb R.K.Porwalb R.K. DayalcL. M.Kuk rej, Pitting corrosion and sensitization in laser rapid manufactured specimens of type 316L stainless steel, Volume 39, August 2012, Pages 509-521.

[5]. N.Parvathavarthinia R.K. Dayala H.S.Khataka V.Shankarb V.Shanmugamb, Sensitization behavior of modified 316N and 316L stainless steel weld metals after complex annealing and stress relieving cycles in the journal of Materials Science Volume 355, Issues 1–3, 1 September 2006, Pages 68-82.

[6]. Shu- XinLiab Lei Lia Shu- Rong Yua R. Akidb Hong- Bo Xiaa, Investigation of intergranular corrosion of 316L stainless steel diffusion bonded joint by electrochemical potentiokinetic reactivation, corrosion science, Volume 53, Issue 1, January 2011, Pages 99-104.

[7]. Kamachi Mudali, M. G. Pujar & R. K. Dayal, Effects of laser surface melting on the pitting resistance of sensitized nitrogen-bearing type 316L stainless steel U, Journal of Materials Engineering and Performance volume 7, pages214–220(1998).

[8]. H. Sidhom, T. Amadou, H. Sahlaoui & C. Braham, Quantitative Evaluation of Aged AISI 316L Stainless Steel Sensitization to Intergranular Corrosion: Comparison Between Microstructural Electrochemical and Analytical Methods, Metallurgical and Materials Transactions A volume 38, pages1269–1280(2007).

[9]. Yong JunOh Jun HwaHong, Nitrogen effect on precipitation and sensitization in cold-worked Type 316L(N) stainless steels, Corrosion science, Volume 278, Issues 2–3, April 2000, Pages 242-250.

[10]. Peter L. AndresenMartin M. Morra, IGSCC of non- sensitized stainless steels in high temperature water, journal of nuclear material, Volume 383, Issues 1–2, 15 Dec 2008.